SPECIAL ISSUE

IUBMB LIFE **WILEY**

# The effects of sulfated hyaluronan in breast, lung and colorectal carcinoma and monocytes/macrophages cells: Its role in angiogenesis and tumor progression

Fiorella M. Spinelli[1] | Paolo Rosales[1] | Stefano Pluda[2] | Daiana L. Vitale[1] | Antonella Icardi[1] | Cristian Guarise[2] | Andrea Reszegi[3] | Ilona Kovalszky[3] | Mariana García[4] | Ina Sevic[1] | Devis Galesso[2] | Laura Alaniz[1] 🔵

[1]Laboratorio de Microambiente Tumoral, CIBA, UNNOBA/CIT NOBA (UNNOBA-UNSADA-CONICET), Jorge Newbery 261, Junín, Argentina

[2]Fidia Farmaceutici S.p.A., Abano Terme, Italy

[3]1st Department of Pathology and Experimental Cancer Research, Semmelweis University, Budapest, Hungary

[4]Laboratorio de Terapia Génica, IIMT – CONICET, Universidad Austral, Derqui-Pilar, Argentina

**Correspondence**
Laura Alaniz, Laboratorio de Microambiente Tumoral, CIBA, UNNOBA/ CIT NOBA (UNNOBA-UNSADA-CONICET), Jorge Newbery 261, Junin, 6000. Bs. As, Argentina.
Email: ldalaniz@comunidad.unnoba.edu.ar

## Abstract

Hyaluronan (HA) is a component of the extracellular matrix (ECM) it is the main non-sulfated glycosaminoglycan able to modulate cell behavior in the healthy and tumor context. Sulfated hyaluronan (sHA) is a biomaterial derived from chemical modifications of HA, since this molecule is not naturally sulfated. The HA sulfation modifies several properties of the native molecule, acquiring antitumor properties in different cancers. In this study, we evaluated the action of sHA of ∼30–60 kDa with different degrees of sulfation (*0.7* sHA1 and *2.5* sHA3) on tumor cells of a breast, lung, and colorectal cancer model and its action on other cells of the tumor microenvironment, such as endothelial and monocytes/macrophage cells. Our data showed that in breast and lung tumor cells, sHA3 is able to modulate cell viability, cytotoxicity, and proliferation, but no effects were observed on colorectal cancer cells. In 3D cultures of breast and lung cancer cells, sHA3 diminished the size of the tumorsphere and modulated total HA levels. In these tumor models, treatment of monocytes/macrophages with sHA3 showed a downregulation of the expression of angiogenic factors. We also observed a decrease in endothelial cell migration and modulation of the hyaluronan-binding protein TSG-6. In the breast in vivo xenograft model, monocytes/macrophages preincubated with sHA1 or sHA3 decreased tumor vasculature, TSG-6 and HA levels. Besides, in silico analysis showed an association of TSG-6, HAS2, and IL-8 with biological processes implicated in the progression of the tumor. *Taken together, our data indicate*

*that sHA in a breast and lung tumor context is able to induce an antiangiogenic action on tumor cells as well as in monocytes/macrophages (Mo/MØ) by modulation of endothelial migration, angiogenic factors, and vessel formation.*

**KEYWORDS**

angiogenesis, monocytes/macrophages, sulfated Hyaluronan, tumor microenvironment

# 1 | INTRODUCTION

Hyaluronan (HA) is a member of the glycosaminoglycan family and is a key component of the extracellular matrix (ECM) of almost all mature tissues.[1] Despite its simple chemical structure, HA can interact with different cellular receptors, binding proteins (such as TSG-6) and proteoglycans.[2,3] These interactions allow HA to regulate various biological processes, such as cell growth, adhesion, migration, and differentiation. Moreover, HA is known to have multiple and complex functions in wound healing, inflammation, and immune responses, as well as in tumoral processes.[4] HA is synthesized by HA synthases and is fragmented into bioactive molecules by hyaluronidases (HAases).[5] It was previously reported that small fragments of HA generated by HAase stimulate angiogenesis,[6] but inhibit tumoral HA signal.[7] Members of the HA signaling pathway, that is, hyaluronan-binding proteins, HA receptors such as CD44, RHAMM, among others, have been shown to promote tumor growth, metastasis, and angiogenesis[4,8] and therefore, HA associated molecules are potential targets for cancer therapy.[9] Chemical derivatives of HA, such as sulfated hyaluronan (sHA), are promising biomaterials since their sulfate groups modulate binding and biological function of native HA. It was previously shown that sulfated HA (sHA) inhibits HAases activity[10] depending on sulfate content and molecular weight.[11] Besides, it was shown that sHA inhibited prostate cancer cell proliferation, motility, and invasion in vitro and abrogated tumor growth in xenograft models.[12] Moreover, in bladder cancer, sHA treatment significantly inhibited tumor growth, probably by inhibiting angiogenesis and HA receptor-PI-3K/AKT signaling.[13] Sulfated HA was also found to be a promising molecule for the treatment of angiogenesis-related disease because it inhibited human umbilical vein endothelial cell (HUVEC) survival and proliferation and human dermal microvascular endothelial cell tube formation.[14] Recently, it was observed that sHA, of low molecular weight (LMW) range and with high sulfation degree, modified breast cancer cell properties with different estrogen receptor status.[15]

Tumor-associated cells such as immune cells and endothelial cells (EC) are essential in the tumor microenvironment.[16] In concert with malignant cells, they allow tumor progression t. One of the most important immune cells of the tumor microenvironment are macrophages (MØ). Tumor-associated MØ (TAMs) play crucial roles in driving growth and progression.[17] In most tumor types, TAMs stimulate the proliferation and migration of tumor cells, promote tumor angiogenesis by high expression of VEGF and remodel the vessel formation.[18] Additionally, HA is able to interact with MØ to induce different intracellular signals depending on its MW.[1,19,20] Besides, we previously determined that HA of high molecular weight (HMW) could induce in monocytes/macrophages (Mo/MØ) an angiogenic potential, associated with the downregulation of TSG-6 expression in a breast cancer model. In contrast, LMW HA did not affect the angiogenic phenotype.[20] For this reason, we decided to evaluate the effects of sHA, with different degrees of sulfation and a MW in the range of LMW, in breast, lung, and colorectal cancer models as well as on EC and Mo/MØ. On the other hand, it is well known that TSG-6 modulates HA function, allowing its crosslinking with other matrix components, therefore modifying the ECM stability and functions.[21] Therefore, we also evaluated if sHA treatments are associated with TSG-6 expression that, in turn, could affect tumoral EC and Mo/MØ cells behavior.

# 2 | MATERIALS AND METHODS

## 2.1 | Reagents

Sulfated hyaluronans (sHA) were synthesized from the tetrabutyl ammonium salt of HA at Fidia Farmaceutici S. p.A.[10,22] For the synthesis of sHA1 and sHA3 (the average number of sulfate groups per disaccharide repeating unit [DS] was 1 and 3, respectively), a $SO_3$-pyridine complex (the molar polymer/$SO_3$ ratio was 1:4 and 1:10, respectively) was used as the sulfation agent in DMSO (20 hr, r.t.). The sulfated products were precipitated in ethanol and purified by dialysis in distilled water, followed by lyophilization. The degree of sulfation was determined by measurements of the sulfur content using ICP-OES (Perkin Elmer) at 181.975 nm (sulfur emission wavelength). sHA1 MW = 28.1 kDa and sHA3 MW = 66.4 kDa. Physicochemical data are shown in Table 1.

## 2.2 | Cell lines

MDA-MB-231 (triple-negative breast adenocarcinoma, ATCC® HTB-26) cells, kindly provided by Roxana Schillaci (IBYME, CABA, Argentina) and LoVo (colorectal adenocarcinoma, ATCC® CCL-229) cells were maintained with DMEM/F12 supplemented with 10% FBS, 2 mM L-glutamine, 100 U/ml streptomycin, and 100 mg/ml penicillin and incubated at 37°C in a 5% $CO_2$ humidified atmosphere. H1299 (Non-small cell lung cancer, ATCC® CRL-5803) cells were maintained with RPMI supplemented with 10% FBS, 2 mM L-glutamine, 100 U/ml streptomycin, and 100 mg/ml penicillin and incubated at 37°C in a 5% $CO_2$ humidified atmosphere. The HMEC-1 (dermal microvascular endothelium) cell line was cultured with DMEM supplemented with 10% FBS, 2 mM L-glutamine, 100 U/ml streptomycin, and 100 mg/ml penicillin and incubated at 37°C in a 5% $CO_2$ humidified atmosphere. In all cell cultures, periodic checkups of cell morphology were performed, as well as strict control of cell line passages (5th–10th passage) and cell line growth rate. In addition, all cell lines were analyzed by PCR to eliminate the presence of mycoplasma contamination.

Confluent cultures of MDA-MB-231, H1299, and LoVo cells were treated with different concentrations of sHA1 and sHA3 for 24 hr. Cell suspensions and conditioned media (CM) were used for experiments. Conditioned media (CM) was collected from supernatants of MDA-MB-231 (MCM), H1299 (HCM), and LoVo (LCM) tumor cell lines cultured ($1.2 \times 10^6$ cells) for 24 hr without serum. The resulting CM was aliquoted and stored at −80°C until use.

## 2.3 | Isolation of PBMC-derived Mo/MØ from human blood

Peripheral blood samples were obtained from voluntary blood donors for isolation of human Mo. Approval was obtained from the Institutional Assessment Committee (CIE)—IRB within the Austral University Hospital (CIE N° 17–006). Informed consent was obtained from participants in accordance with the Declaration of Helsinki.

PBMC-derived Mo/MØ were isolated from healthy donors′ blood by the Ficoll-Paque Plus (GE Healthcare) gradient, followed by a Percoll gradient to enrich it with Mo. Cells were plated into 12-well plates for 2 hr, and nonadherent cells were removed. Then, adhered cells were subsequently cultured overnight in complete RPMI 1640 medium.[23] Twenty-four hours later, the medium of the adherent Mo/MØ was replaced with RPMI 1640 (FBS free) and treated with sHA1 (100 μg/ml), sHA3 (100 μg/ml) or conditioned media from MDA-MB-231 (MCM), H1299 (HCM), and LoVo (LCM) cells. After 24 hr, the cells were centrifuged and used for experiments.

## 2.4 | MTS

Cell viability was measured by MTS assay (Abcam ab197010) as described in the manufacturer′s protocol. MDA-MB-231, H1299, LoVo, HMEC-1 or Mo/MØ cells were seeded in 96-well plates at a density of $6 \times 10^3$ cells per well and treated with sHA1 or sHA3 (0, 20, 100 and 1,000 μg/ml). Three hours before the treatments ended, MTS dye was added and incubated for 3 hr in the dark. The optical density (OD) values were measured at 490 nm.

## 2.5 | Cytotoxicity assay

To measure cytotoxicity, liberation of LDH was measured by cytotoxicity assay kit (Abcam ab65391). MDA-MB-231, H1299, and LoVo cells were plated at $2 \times 10^4$ cells per well and incubated at 37°C in 5% $CO_2$ until they stabilized and then were treated with sHA (0, 20, 100, and 1,000 μg/ml). Every treatment was evaluated in triplicate, and the following controls were performed: background control, low control and high control (with 1% Triton

**TABLE 1** Physicochemical data of sHA1 and sHA3

| Derivative | Degree of sulfation | Molecular weight of disaccharide repeating unit | Weight average molecular weight MW | Intrinsic viscosity IV | Hydrodynamic radius Rh |
|---|---|---|---|---|---|
| Id. Batch cod | Eq. SO₄Na/Eq. disaccharide repeating unit | Da | kDa | Dl/g | Nm |
| sHA1 (batch RS015/16) | 0.7 | 477 | 28.1 | 1.1 | 7.5 |
| sHA3 | 2.5 | 661 | 66.4 | 0.7 | 8.5 |

*Note*: Batch RS010/16.

X-100). Then, the assay was carried out according to the instructions provided by the manufacturer.

## 2.6 | Proliferation assay

The thymidine incorporation assay uses the strategy of incorporating the radioactive nucleoside 3H-thymidine into new strands of chromosomal DNA during mitotic cell division. The radioactivity in DNA recovered from the cells was measured to determine cell proliferation. Briefly, $2 \times 10^4$ MDA-MB-231, H1299 or LoVo cells were seeded in 96-well plate, incubated for 24 hr for adhesion and then treated with sHA1 or sHA3 (100 μg/ml) for 24 hr. Six hours before the end of treatment, the cells were treated with 3H-thymidine (0.8 μCi/well). Once the treatment ended, the cells were collected with a cell harvester, and radioactive DNA was measured with a scintillation beta-counter.

## 2.7 | Apoptosis

To analyze whether sHA treatment induced apoptosis in tumor cells, Annexin V-APC and propidium iodide (ImmunoTools) were analyzed by flow cytometry. Briefly, $5 \times 10^5$ MDA-MDB-231, H1299 or LoVo cells were treated with sHA1 or sHA3 (100 μg/ml) according to the instructions provided by the manufacturer. As a positive control, apoptosis and necrosis were induced with 4% PFA, and cells without treatment and without dye were used as autofluorescence controls. Samples were processed by FACSCanto II, and data were analyzed using FlowJo (LCC).

## 2.8 | Three-dimensional spheroid culture

Hanging drops were made with $1.2 \times 10^4$ MDA-MB-231, H1299 or LoVo cells in 30 μl of complete medium with or without sHA1 or sHA3 (100 μg/ml). The hanging drops were incubated in standard culture conditions for 10 days.[24] Images of the spheroids in every condition were captured, and the area of each one was measured using ImageJ 1.50b software. Spheroids were fixed with methanol and incubated with HA-binding protein (385,911, Calbiochem). The spheroids were washed and incubated for 2 hr with streptavidin conjugated with FITC (31274243, Immunotools) and then were rinsed with PBS and labeled with DAPI (0.3 μg/ml). Images of the stained sections were taken with a Nikon Eclipse E800 fluorescence microscope and quantified with ImageJ.

## 2.9 | HA ELISA like assay

The protocol used to detect the soluble fraction of HA was adapted from previous studies[24] and developed by our laboratory. A specific HA-binding protein (HABP) was used to cover a 96-well plate. Then, MDA-MB-231, H1299, LoVo or Mo/MØ cell supernatant samples were plated, and HABP protein was added in its biotinylated form to determine the concentration of HA through colorimetric detection of peroxidase enzyme activity. Optical density was detected by a spectrophotometer at 450 nm.

## 2.10 | RT-qPCR

Total RNA was extracted by Tri Reagent (TR 118, Molecular Research Center, Inc.). RNA quantification was evaluated by spectrophotometry. Then, 2 μg of RNA was reverse transcribed with 200 U of RT M-MLV Reverse Transcriptase (M1701, Promega) and 2.5 pmol/μl of oligo (dT) primers (GenBiotech). cDNAs were then subjected to real-time quantitative PCR (RT-qPCR) using FastStart SYBR Green Master Mix (04673484001, Roche) and 200 nM of each specific primer (Invitrogen, Life Technologies™):

VEGF: forward 5′-CTCCTCCACCATGCCAAGT-3′ and reverse 5′-GCAGTAGCTGCGCTGATAGA-3′;
IL-8: forward 5′-AAGGAAAACTGGGTGCAGAG-3′ and reverse 5′-GGCATCTTCACTGATTCTTGG-3′;
FGF-2: forward 5′-CCTGGCTATGAAGGAAGATGG-3′ and reverse 5′-TCGTTTCAGTGCCACATACC-3′;
GAPDH: forward 5′-GGGGCTGCCCAGAACATCAT-3′ and reverse 5′-GCCTGCTTCACCACCTTCTTG-3′; and
β2-microglobulin: forward 5′-CACCCCCACTGAAAAAG ATG-3′ and reverse 5′-CTTACCTCCATGATGCTGCTTA C-3′.

The PCR conditions were as follows: 90 s at 94°C and then 40 cycles of 30 s at 94°C, 30 s at 60°C and 30 s at 72°C. Values were normalized to the levels of the GAPDH housekeeping gene.

## 2.11 | ELISA

ELISAs were used to detect the protein levels of VEGF (DY293B, R&D Systems™) in MDA-MB-231, H1299 or LoVo conditioned media and total TGF-β1 (436707, Legend Max, BioLegend), active TGF-β1 (437707, Legend Max, BioLegend), and IL-1β (DY201-05, R&D Systems™) in cell-free conditioned media of Mo/MØ. The assays were carried out according to the instructions provided by the manufacturer.

## 2.12 | Western blotting

To analyze TSG-6 biosynthesis in the supernatants of Mo/MØ, equal amounts of protein were resolved by 0.1% SDS-10% polyacrylamide gel denaturing electrophoresis (SDS-PAGE) and transferred to nitrocellulose membranes. The membranes were incubated overnight at 4°C with RAH-1, a polyclonal human TSG-6 antibody (dilution 1/5000)[25] (kindly supplied by Dr. Anthony Day), and then incubated for 1 hr at RT with horseradish peroxidase-labeled secondary antibody. Finally, the HRP chemiluminescence reaction was detected using a stable peroxide solution and an enhanced luminol solution. Images were obtained with an ImageQuant 4000 mini bioluminescent image analyzer (GE HealthCare Life Sciences) and analyzed using ImageJ.

## 2.13 | In vitro endothelial and Mo/MØ cell migration assay

In vitro migration was performed using a 48-well Transwell microchemotaxis Boyden Chamber unit (Neuroprobe, Inc.). HMEC-1 cells or Mo/MØ ($1.5 \times 10^3$ cells/well) were placed in the upper chamber, and conditioned medium of the treatments was applied to the lower chamber of the Transwell unit. As a negative control, cells were exposed to DMEM and RPMI without FBS, and as a positive control, a medium rich in angiogenic factors was used. The chamber was left for 4 hr at 37°C in a 5% $CO_2$ humidified atmosphere. Cells attached to the lower side of the membrane were fixed in 2% formaldehyde and stained with 4′,6-diamidino-2-phenylindole dihydrochloride (DAPI, Sigma-Aldrich). Images from three representative visual fields were captured using a Nikon Eclipse E800 fluorescence microscope and were analyzed using CellProfiler software (www.cellprofiler.com), and the mean number of cells/fields ± SEM was calculated.

## 2.14 | Tumor xenograft model

Six- to eight-week-old male nu/nu mice were purchased from Comisión Nacional de Energía Atómica, Ezeiza, Buenos Aires, Argentina. Animals were maintained at our Animal Resources Facilities (CIBA, CIT NOBA) following the experimental ethical committee and the NIH Guide for the Care and Use of Laboratory Animals (eighth edition). An MDA-MB-231 or H1299 cell suspension ($1 \times 10^7$ cells/0.1 ml) was injected subcutaneously into the dorsal flank of mice. After, 9 days, PBMC-derived Mo/MØ treated or not with sHA1 or sHA3 were inoculated subcutaneously near the base of the tumor. On day 29, mice were sacrificed, and tumors were removed, fixed in 10% formalin and embedded in paraffin. Before staining, 3-μm sections were deparaffinized and dehydrated.

## 2.15 | Vasculature detection in tumor tissues

Slides were rinsed with PBS and labeled with DAPI (0.3 μg/ml) plus 20 μg/ml of fluorescein-labeled Griffonia (Bandeiraea) Simplicifolia Lectin I (GSL I; FL-1101, Vector Laboratories) that binds specifically to endothelial cells in mouse tissues.[26] The sections were rinsed with PBS and mounted on microscope slides. Images of the stained sections were taken with a Nikon Eclipse E800 fluorescence microscope. Microvessels were quantified with ImageJ software.

## 2.16 | Immunostaining of TSG-6 and HA in tumor tissues

Slides were rinsed with PBS and incubated overnight at 4°C with rabbit anti-human polyclonal antibody against TSG-6 (RAH-1) (dilution 1/1,000)[25] and HA binding protein conjugated with avidin (385911, Calbiochem). Afterward, the tissue slices were washed three times in PBS and then incubated for 1 hr at 4°C with secondary rabbit antibody conjugated with Texas Red® (TI-1000, Vector Laboratories) and streptavidin conjugated with FITC (31274243, Immunotools). The sections were rinsed with PBS, stained with DAPI (0.3 μg/ml) and then mounted on microscope slides. Images of the stained sections were taken with a Nikon Eclipse E800 fluorescence microscope and quantified with ImageJ.

## 2.17 | Protein–protein interaction analysis

STRING v11 (http://string-db.org/) was used to develop in silico protein interaction networks for TSG-6. All interactions were predicted with a high confidence threshold of 0.700. Additionally, for the enrichment analysis, STRING uses three different databases: GO, Pfam (Protein families), and KEGG and performs a multiple testing correction separately within each functional classification framework (GO, KEGG, InterPro, etc.), according to Benjamini and Hochberg, to predict protein–protein interaction (PPI) networks.[27]

## 2.18 | Statistical analysis

For statistical analysis, 95% confidence intervals (CIs) were determined by calculating arithmetic mean values and variance (standard deviation, SD) of three independent experiments. To evaluate whether differences between the obtained values were significant, analysis of variance (ANOVA, Tukey's test) was used in case of the experiments with more than two experimental groups. Prism software (GraphPad, San Diego, CA, USA) was used, considering a $p$ value <.05 as statistically significant.

## 3 | RESULTS

### 3.1 | sHA effects on tumor and associated cells survival

First, we assessed viability, cytotoxicity, apoptosis, and proliferation action of sHA1 and sHA3 at different concentrations (20, 100, and 1,000 μg/ml) on MDA-MB-231, H1299, and LoVo tumor cell lines, endothelial cell line, HMEC-1 and Mo/MØ derived from human peripheral blood. In the triple negative (TN) breast cancer cell line MDA-MB-231 we observed that sHA1 decreased cell
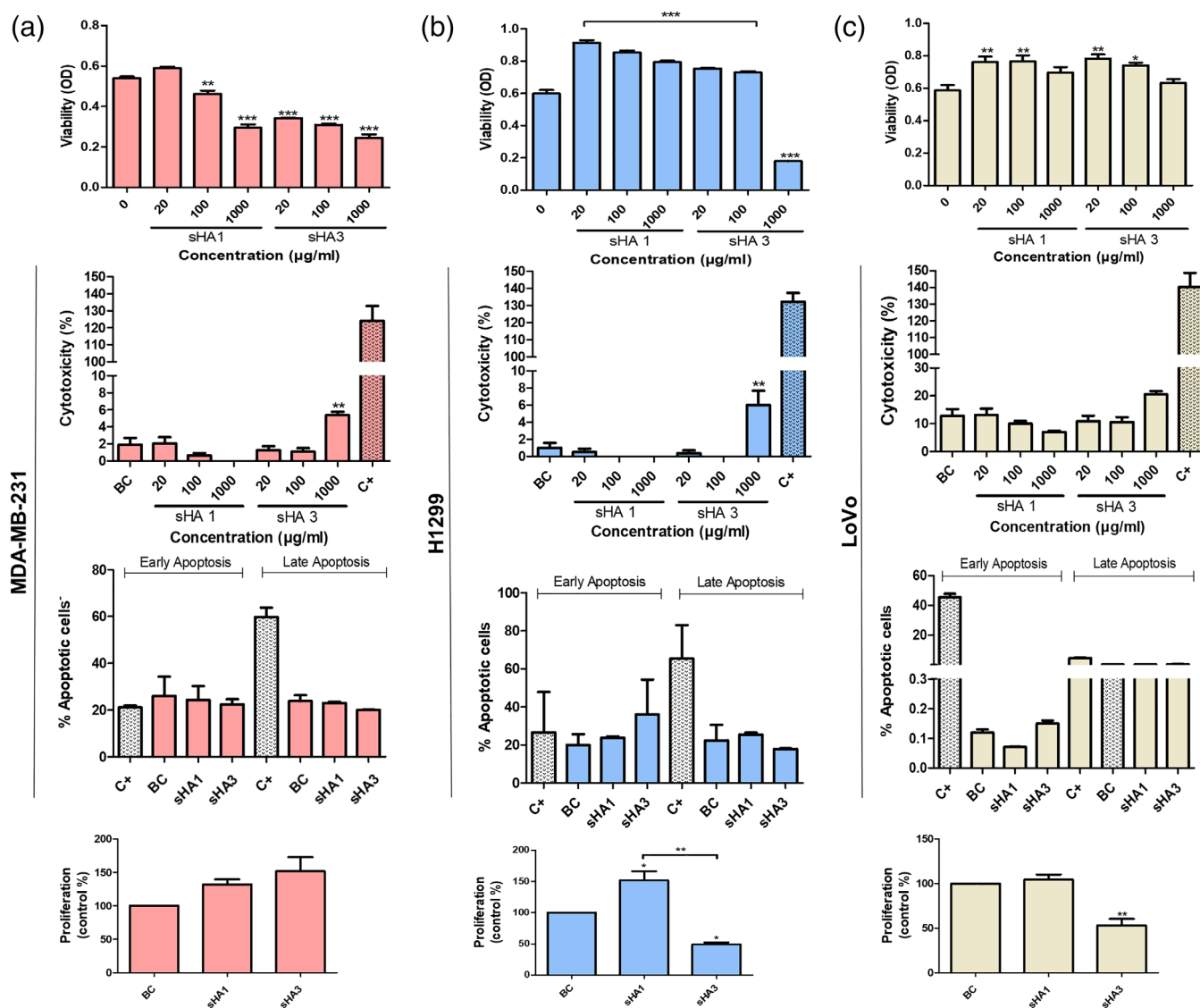


**FIGURE 1** Cell viability, cytotoxicity, apoptosis, and proliferation on MDA-MB-231 (a), H1299 (b) and LoVo (c) cells under different concentrations of sHA1 and sHA3 (μg/ml). Cell viability was performed with the MTS assay. Cytotoxicity was measured LDH liberation in colorimetric assay (C+ positive control). Apoptosis was evaluated by Annexin V in flow cytometry assay, which determined early and late apoptotic events. Proliferation was measured by thymidine incorporation assay. (*) $p < .05$, (**) $p < .01$, (***) $p < .001$, regard to basal control (BC)

viability significantly at the concentration of 100–1,000 µg/ml whereas sHA3 decreased cell viability at every concentration tested (20–1,000 µg/ml); with these data, the IC50 was calculated for sHA1 and sHA3, being 189.3 ± 0.13 µg/ml for sHA1 and 112.3 ± 0.39 µg/ml for sHA3 (Figure S1). Moreover, sHA3 at its higher concentration caused cytotoxicity. On the other hand, we found that sHA did not induce apoptosis or modify the proliferation rate of this cells (Figure 1a). Contrary to the non-small cell lung cancer cell line H1299, we found that sHA1 at every concentration tested and sHA3 at the concentration of 20 and 100 µg/ml increased cell viability, but sHA3 decreased cell viability and induced cytotoxicity at its higher concentration. None of the sHA species caused apoptosis. However in this cell line, sHA3 (100 µg/ml) significantly decreased the proliferation rate, whereas SHA1 enhanced the proliferation (Figure 1b), indicating that in these cells only sHA3 can reduce cell survival. On the other hand, in the colorectal cancer cell line Lovo, both sHA increased cell viability at 20 and 100 µg/ml. None of the sHA species induced cytotoxicity or apoptosis, but sHA3 (100 µg/ml) significantly decreased the proliferation rate (Figure 1c). Indicating that in these cells, sHA3 are able to reduce cell proliferation.

Considering these results, we decided to treat tumor cell lines with sHA1 or sHA3 at a concentration of 100 µg/ml, because it was lower than the IC50, and that concentration did not induce significant cytotoxicity.

Additionally, we also evaluated the effect of sHA on the viability of endothelial cells (HMEC-1) and Mo/MØ derived from human peripheral blood. In the case of endothelial cells, we observed that sHA1 or sHA3 did not affect the viability of HMEC-1 cells at any assessed concentration (Figure S2a). However, sHA1 or sHA3 increased the cell viability of Mo/MØ (Figure S2b). Taking into account these results, we decided to treat these cells with the same sHA concentration used with tumor cells (100 µg/ml).

From these results, we conclude that sHA affects cancer cell death depending on the cell type by inducing molecular mechanisms of death other than apoptosis.
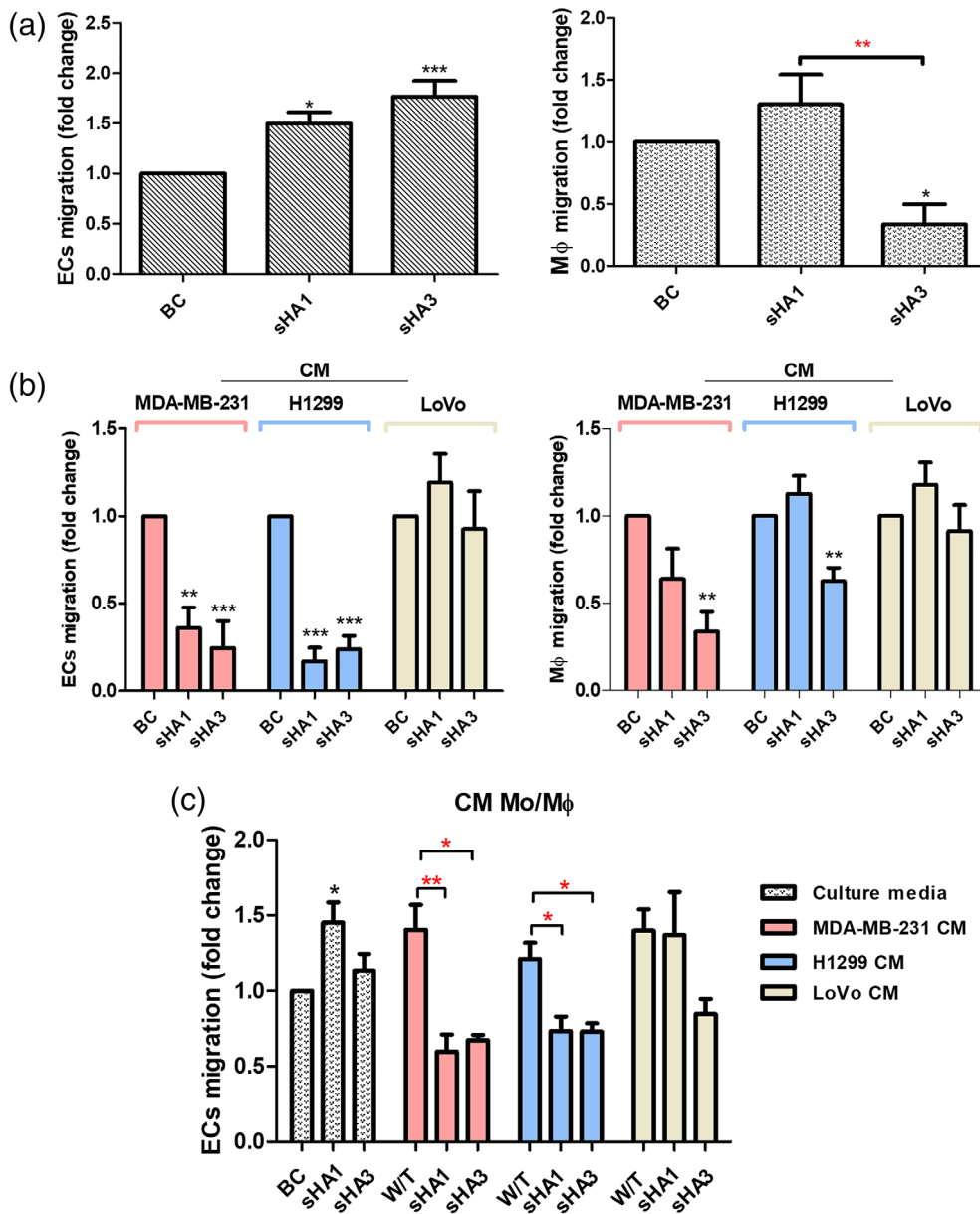
## 3.2 | In vitro cell migration of HMEC-1 cells and Mo/MØ

Previous studies reported that sHA has antiangiogenic action.[28] Thus, we decided to analyze, first, endothelial cell (EC) migration levels towards (a) sHA1 or sHA3, (b) the conditioned media (CM) of MDA-MB-231 (MCM), H1299 (HCM), and LoVo (LCM) cells treated with sHA or (c) CM of Mo/MØ treated with sHA with or without

CM of tumor cells; and to take into account a tumor-free context and a tumor context associated or not with the presence of Mo/MØ. Secondly, Mo/MØ migration levels towards (a) sHA1 or sHA3 and (b) CM MDA-MB-231, H1299 and LoVo cells treated with sHA. sHA1 or sHA3 significantly increased the migration of ECs in comparison to cell culture media in a tumor-free context. (Figure 2a). However, sHA3 significantly decreased the migration of Mo/MØ in comparison to cell culture media. On the other hand, in a tumor context, CM of MDA-MB-231 and H1299 cells treated with sHA1 or sHA3 decreased EC chemotaxis, compared to BC (CM of cells without treatment) (Figure 2b). Nevertheless, CM of LoVo cells treated with sHA1 or sHA3 did not affect EC chemotaxis (Figure 2a). In the case of Mo/MØ, we observed a decrease in cell migration toward CM of MDA-MB-231 and H1299 cells treated with sHA3 (Figure 2b). However, CM of LoVo cells treated with sHA1 or sHA3 did not modulate Mo/MØ migration levels (Figure 2b). When we evaluated EC migration toward CM of Mo/MØ, we observed, first, that EC chemotaxis increased with CM of Mo/MØ treated with sHA1 (Figure 2c) compared to BC (CM of cells without treatment). However, in a tumor context EC chemotaxis decreased with CM of Mo/MØ treated with CM of MDA-MB-231 and H1299 treated with sHA1 or sHA3 (Figure 2c) compared to CM of MDA-MB-231 and H1299 without treatment. Nevertheless, CM of Mo/MØ treated with CM of LoVo cells treated with sHA1 or sHA3 did not affect EC migration levels significantly (Figure 2c). This indicated that the sHA has a differential effect in a tumoral microenvironment compared to a physiological milieu.

## 3.3 | Detection of Angiogenic factors in tumor cells and Mo/MØ

Consequently, we decided to evaluate which angiogenic factors decreased EC and Mo/MØ migration levels triggered by sHA in the tumor context. We evaluated VEGF levels in MDA-MB-231, H1299, and LoVo supernatants and found a significant decrease with sHA3 treatment only in MDA-MB-231 supernatants (Figure 3a). Furthermore, it is well known that Mo/MØ induce tumor vascularization by secreting angiogenic factors, such as VEGF, IL-8, and FGF-2. We evaluated the mRNA expression levels of these factors in Mo/MØ treated with sHA with or without CM of MDA-MB-231 and H1299. We observed that the CM of these cell lines treated with sHA3 reduces the VEGF, IL-8, and FGF-2 mRNA expression to undetectable levels, being variable in the case of sHA1 treatment. Similarly, sHA inhibited the mRNA

FIGURE 2 In vitro cell migration of endothelial cells (ECs) and Mo/MØ in physiological and tumor contexts. Migration toward to culture media with or without sHA (a) and conditioned media of tumor cells treated with sHA1 or sHA3 (b). ECs migrated to conditioned media of Mo/MØ treated with sHA1 or sHA3 and conditioned media of tumor cells plus sHA1 or sHA3 (c). Results are expressed as an index of cell migration with respect to non-treated basal control (BC) $\pm$ SEM from three representative visual fields. The results are representative of three independent experiments: (*) $p < .05$, (**) $p < .01$, (***) $p < .001$. Black asterisks indicate significant differences regard to BC; red asterisks indicate significant differences between treatments. CM, conditioned media; W/T, without treatment

expression in physiological conditions (culture media; Figure 3b,c).

## 3.4 | Cytokines profile of Mo/MØ

Since it is important to define the phenotype that Mo/MØ acquired in the tumor environment, we decided to evaluate whether sHA could modulate the biosynthesis of key anti- or proinflammatory cytokines TGF-1β and IL-1β in Mo/MØ (Figure 4a,b). We observed a significant reduction of total TGF-1β in Mo/MØ previously exposed to CM of MDA-MB-231, a similar tendency was observed for the other cell lines. Regarding the modulation of IL-1β, we could not detect significant changes in Mo/MØ

previously exposed to CM of MDA-MB-231 and H1299, contrary in Mo/MØ previously exposed to CM of Lovo cells, where we observed a significant reduction of these cytokines (Figure 4c).

## 3.5 | Soluble HA levels in tumor cells and Mo/MØ

Because it was reported that sHA modulates HA metabolism, synthesis, and degradation, acting as hyaluronidases inhibitor[11] we decided to analyze the content of HA secreted by MDA-MB-231, H1299 and LoVo cells and Mo/MØ in a physiological and tumor context. In the case of Mo/MØ, sHA did not modulate soluble HA levels in a
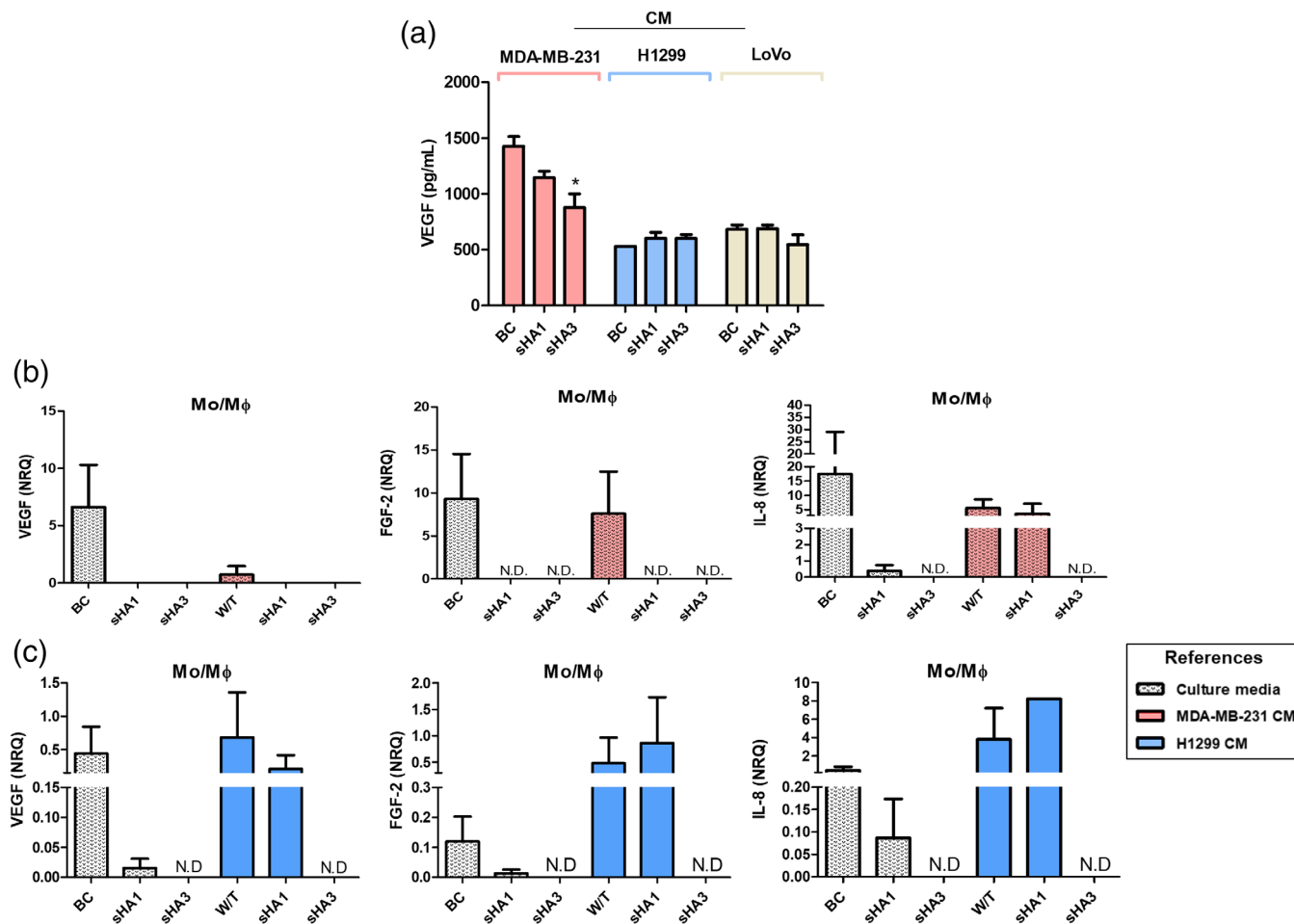
**FIGURE 3** VEGF protein expression and mRNA levels of proangiogenic factors in Mo/MØ treated with sHA1 or sHA3 in physiological and tumor contexts. VEGF levels in supernatants of MDA-MB-231, H1299, and LoVo cells, treated or not with sHA1 or sHA3, measured by ELISA (a). Data are expressed as mean ± SEM of VEGF levels (pg/ml) from three independent experiments. VEGF, FGF-2 and IL-8 mRNA levels measured by RT-qPCR, in Mo/MØ treated or not with sHA1 or sHA3 in physiological and breast (b) or lung (c) contexts. Data are expressed as normalized relative quantities (NRQ) mean ± SEM from three independent experiments. (*) $p < .05$, (**) $p < .01$, (***) $p < .001$. Black asterisks indicate significant differences with respect to basal control (BC). CM, conditioned media; W/T, without treatment

physiological context (culture media). However, it increased significantly with CM derived from MDA-MB-231 treated or not with sHA3 and from LoVo treated or not with sHA3 (Figure 5a) with respect to culture media (basal control: BC). CM from H1299 cells treated or not with sHA did not modulate Mo/MØ soluble HA levels (Figure 5a) with respect to culture media (BC). Surprisingly, CM from MDA-MB-231 and H1299 treated with sHA1 reduced Mo/MØ soluble HA levels with respect to CM without treatment (W/T), respectively. Besides, CM of LoVo treated with sHA1 decreased Mo/MØ soluble HA levels with respect to CM from LoVo W/T (Figure 5a). On the other hand, we did not observe significant differences in the soluble HA levels, between treatments, in any tumor cell line (Figure 5b). Thus, we could observe that only sHA1 could reduce the HA levels in Mo/MØ in all tumor contexts.

## 3.6 | 3D tumor culture, spheroid size, and HA levels

Tumor cells in vivo form 3D structures that are essential to interact with the surrounding ECM, thus it is a better model to study the impact of ECM on tumor cell behavior.[24] Therefore, we decided to culture MDA-MB-231, H1299 and LoVo cells in 3D, using the hanging drop technique, and evaluate spheroids size and total HA levels. sHA1 treatment did not affect mammosphere size, however, sHA3 treatment reduced tumorsphere size (Figure 6a, b, top panel). At the same time, sHA1 and sHA3 treatment reduced H1299 spheroids size (Figure 6a,b, middle panel). Nonetheless, sHA1 or sHA3 treatment did not affect LoVo spheroids size (Figure 6a,b, bottom panel).

On the other hand, sHA3 treatment increased total HA levels of MDA-MB-231 with respect to basal control
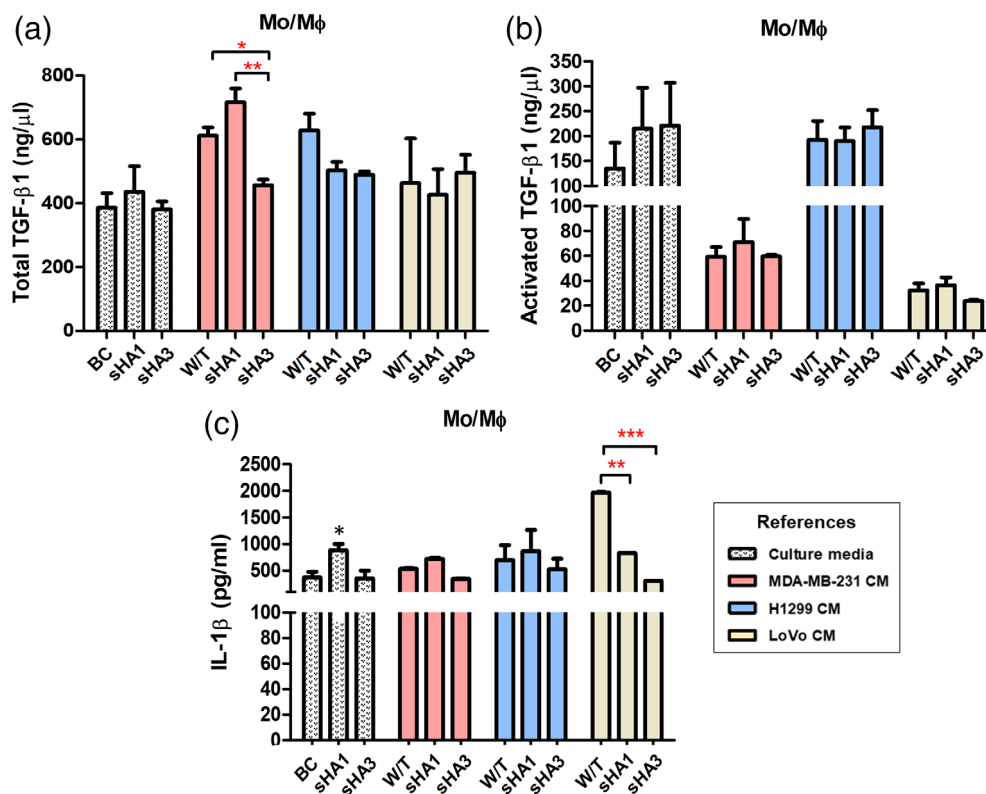
**FIGURE 4** Cytokine protein expression from supernatants Mo/MØ treated with sHA1 or sHA3 in physiological and tumor context. Total TGF-β1 (a), activated TGF-β1(b) and IL-1β (c). Data are expressed as mean ± SEM of cytokines levels (ng/μl; pg/ml) from three ELISA independent experiments. (*) $p < .05$, (**) $p < .01$, (***) $p < .001$. Black asterisks indicate significant differences with respect to basal control (BC); red asterisks indicate significant differences between treatments. CM, conditioned media; W/T, without treatment

and sHA1 treatment (Figure 6c). Otherwise, sHA1 treatment significantly increased total HA levels of H1299, with respect to basal control, however, sHA3 decreased total HA levels of H1299 with respect to basal control and sHA1 treatment (Figure 6c). None of the sHA treatments modulated total HA levels of LoVo cells (Figure 6c) with respect to basal control.

## 3.7 | TSG-6 protein expression in Mo/MØ in a breast tumor context and sHA treatment

We previously reported that HA could modulate TSG-6, a hyaluronan-binding protein, in Mo/MØ in a breast tumor context, and this was associated with a reduction of the angiogenic behavior of these cells.[20] Therefore, we used western blot to evaluate the protein expression levels of TSG-6 in supernatants of Mo/MØ treated with sHA. We detected two species: (a) ∼ 35 kDa corresponding to free TSG-6 and (b) ∼ 120 kDa corresponding to the complex generated by the heavy chain (HC) of IαI and TSG-6, as has been documented by other authors.[25] We detected that sHA1 significantly increased the TSG-6−35 kDa species corresponding to free TSG-6 compared to basal condition and sHA3. Besides, similar results were observed in experimental conditions with MCM and MCM plus sHA3 (Figure 7a). However, the ∼120 kDa species,

corresponding to TSG-6·HC that was only detected in the tumor context, has a tendency to increase with the treatment of MCM plus sHA3 and to decrease with MCM plus sHA1 (Figure 7a). This indicates that, sHA could modify the enzymatic activity of TSG-6 depending on the sulfated grade.

## 3.8 | Effect of Mo/MØ preincubated with sHA1 or sHA3 on xenograft breast cancer model

Nu/nu mice were injected with MDA-MB-231 cells, and 9 days later, animals with similar tumor volumes were inoculated with Mo/MØ preincubated with sHA1 or sHA3. Tumor volume was measured weekly, and we found no differences in tumor growth between treatments (data not shown). Tumors were fixed, and sections were stained with: (a) H&E to rule out changes in tumor histology, (b) TSG-6, (3) HA, and (4) GSL-1 to analyze ECs forming blood vessels.

Mice inoculated with Mo/MØ preincubated with sHA1 or sHA3 exhibited significantly decreased TSG-6 immunofluorescence intensity compared to mice inoculated with Mo/MØ without treatment (Figure 7b). Additionally, these treatments reduced the immunofluorescence intensity levels of HA when compared to tumor controls and Mo/MØ control (Figure 7b).
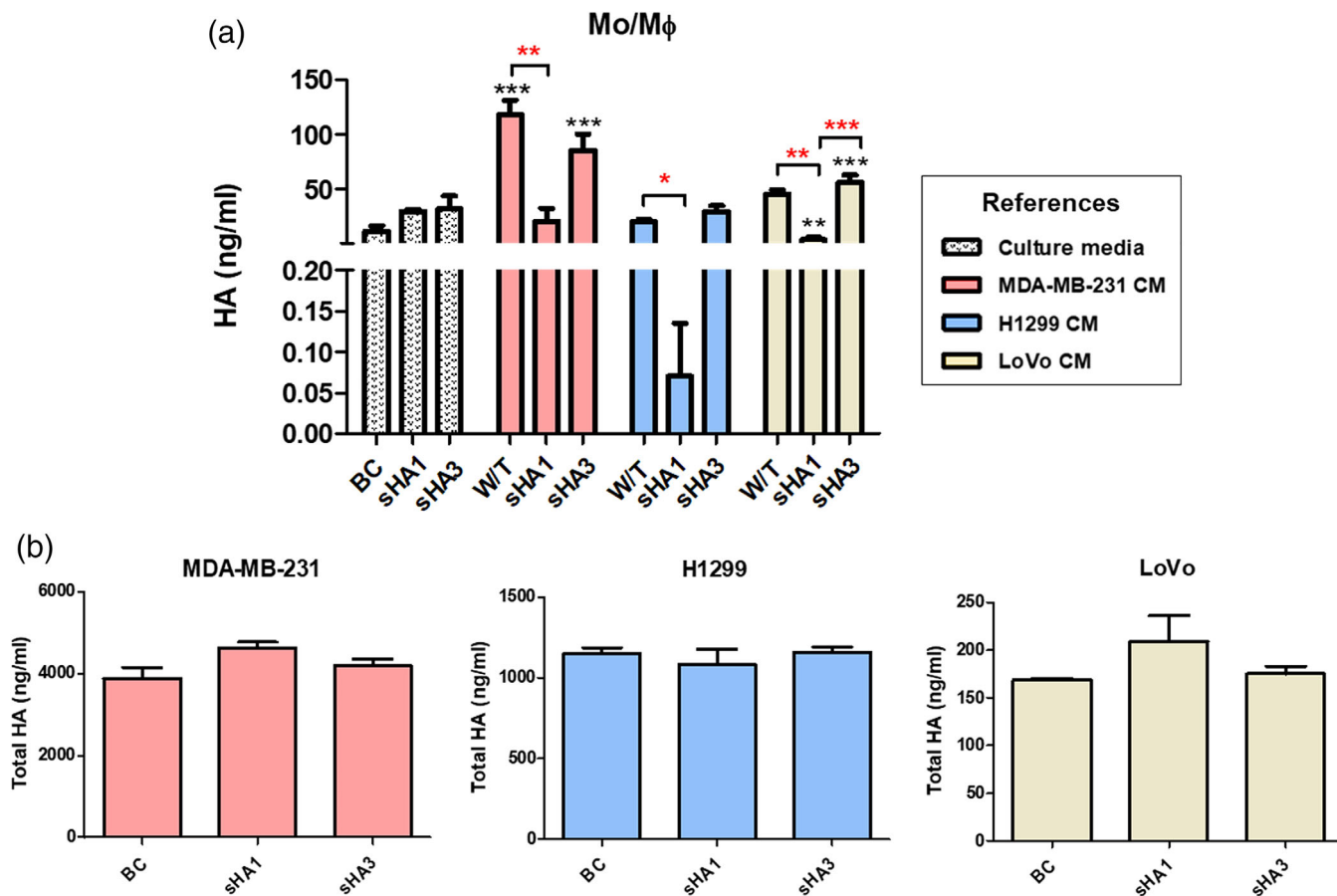
**FIGURE 5** HA levels, measured by ELISA, in supernatants of Mo/MØ treated or not with sHA1 or sHA3 in physiological and tumor contexts (a) and MDA-MB-231, H1299 and LoVo cells treated or not with sHA1 or sHA3 (b). Data are expressed as mean ± SEM of HA levels (ng/ml) from three independent experiments. (*) $p < .05$, (**) $p < .01$, (***) $p < .001$. Black asterisks indicate significant differences regard to basal control (BC); red asterisks indicate significant differences between treatments. CM, conditioned media; W/T, without treatment

Mo/MØ preincubated with sHA1 or sHA3 induced a significant decrease in the tumor vasculature in the MDA-MB-231 model detected by immunofluorescence intensity (AU) of GSL-1-FITC in comparison to the tumor control as well as those animals inoculated with Mo/MØ without treatment (Figure 8a). These in vivo data are in concordance with the in vitro results, indicating that sHA modulate the angiogenic behavior of Mo/MØ, probably through modulation of TSG-6 and HA levels.

## 3.9 | In silico protein–protein interactions analysis of TSG-6 implicated in tumor inflammation, blood vessel morphogenesis, and cancer

To explain the observed results about the modulation of TSG-6 by sHA we perform an in silico protein

interaction network analysis associated with TSG-6, using the STRING (Search Tool for the Retrieval of Interacting Genes/Proteins) online tool.[27] The analysis showed that TSG-6 interacts directly or indirectly with CCL5, CXCL8 (IL-8), CXCL11, ITIH4 (inter-alpha-trypsin inhibitor heavy chain H4) and PTX3 (Pentraxin-related protein), proteins involved in immune responses, inflammatory reactions, and cell chemotaxis. Besides, TSG-6 interacts with other components of ECM like THBS1 (Thrombospondin-1) and FN1 (Fibronectin type III) and with HA synthase 2 (Figure 8a). Then we analyzed biological processes, WikiPathways, molecular functions and KEGG pathways related to this network. Because of the enrichment of biological processes, the red was associated with inflammatory response, cell migration and proliferation, cell adhesion and chemotaxis of monocytes and other blood cells, responses to cytokines and chemokines, blood vessels morphogenesis and HA metabolism (Figure 8b, green bars). We also
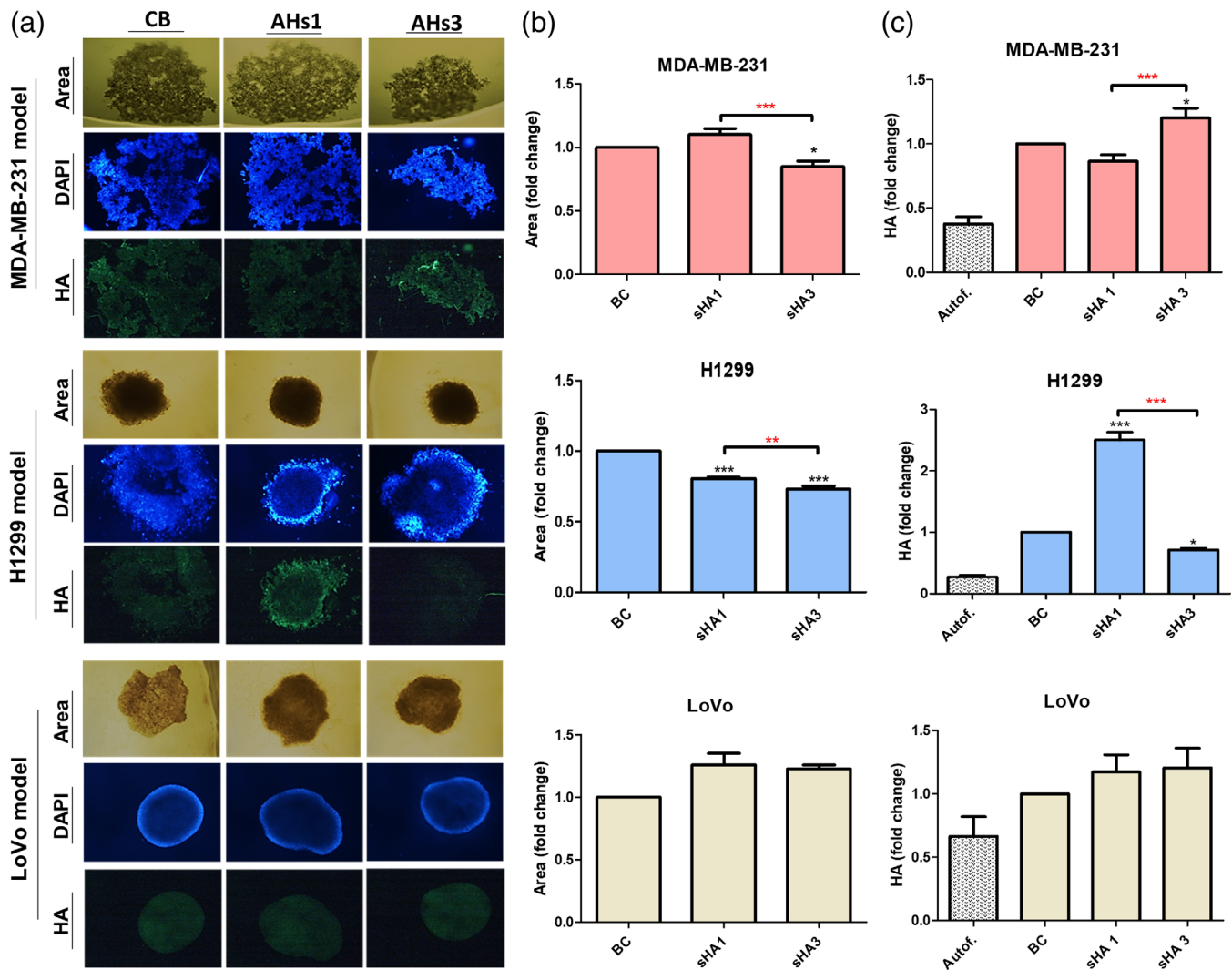
**FIGURE 6** In vitro 3D growing of MDA-MB-231, H1299 and LoVo cells, treated or not with sHA1 or sHA3. Left to right panels: images of spheroids observed with light microscope and fluorescence microscope (100×) (a), spheroids area (b) and HA levels analysis (c), of each cell lines treated with sHA1 or sHA3. Data are expressed as fold change of spheroids area and HA levels from three independent experiments. (*) $p < .05$, (**) $p < .01$, (***) $p < .001$. Black asterisks indicate significant differences regard to basal control (BC); red asterisks indicate significant differences between treatments

observed some of these functions in the molecular function group (Figure 8d, orange bars). In Wiki and KEGG pathways, we found that TSG-6 and related proteins were associated with inflammatory response pathways like toll-like receptor and IL-18 signaling pathway and cytokine–cytokine receptor interaction, senescence and autophagy in cancer and lung fibrosis (Figure 8c,f, blue and yellow bars, respectively). Moreover, we used STRING to predict the association between the analyzed target network based on PubMed co-citation references and the following key articles were found connected to inflammation and ECM in tumor microenvironment, hyaluronan, monocyte/macrophage differentiation, regulation of chemokine function, and others (Figure 8d, violet bars).

## 4 | DISCUSSION

Our work has examined the action of sHA in TN breast, lung, and colorectal models, and its impact in associated cells of the tumor microenvironment, such as endothelial and the monocyte/macrophage immune cells. As mentioned above, it was previously shown that sHA reduced tumor aggressiveness in several cancer models as bladder, prostate, and breast cancer.[12–15] However, no reports were found about action on tumor-associated cells, which was evaluated in our study. It is important to note that sHA action is dependent on sulfation degree, thus our first objective was to assess if the sHA1 and sHA3 sHA as LMW or fragments, with different sulfation degrees but similar MW range 30–60 kDa (around 60–100 monomers,
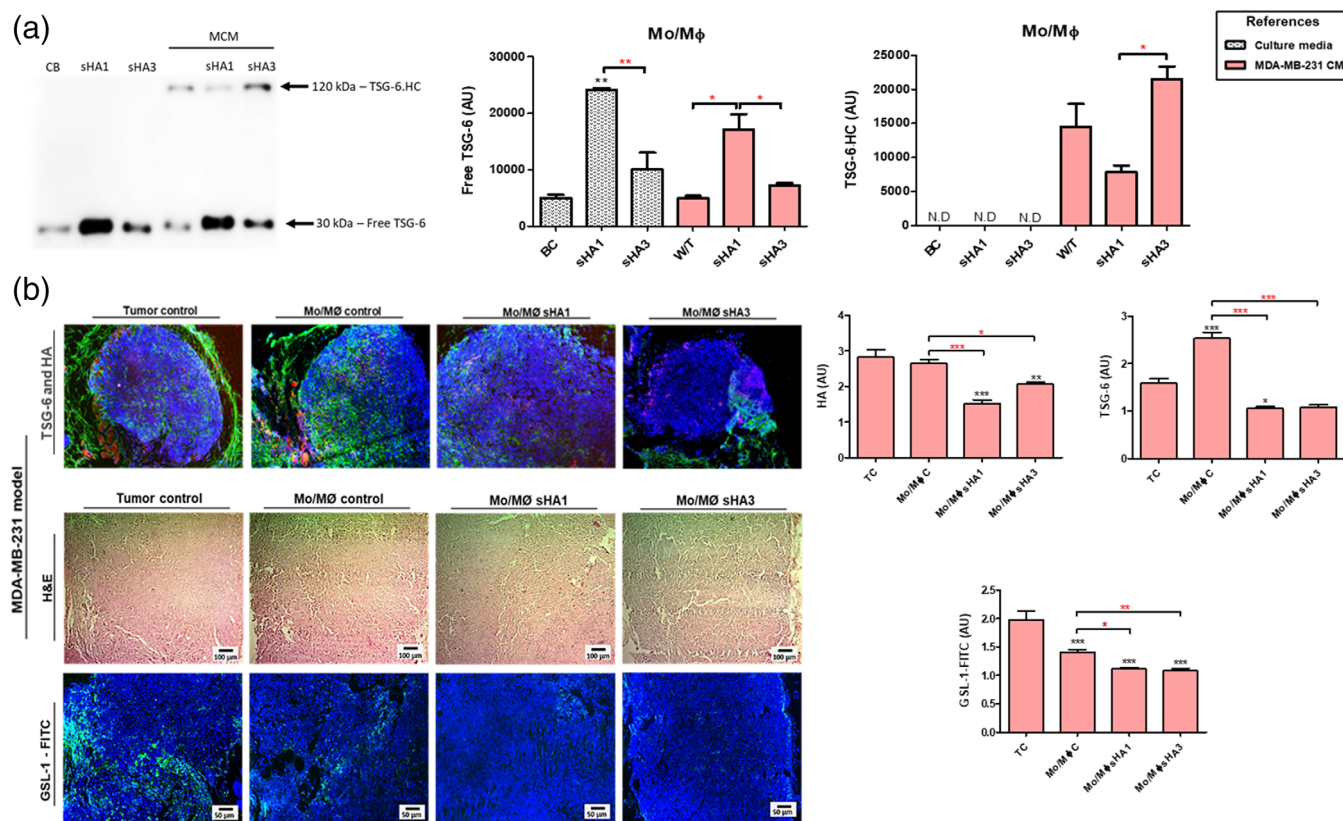
**FIGURE 7** TSG-6 expression modulation in Mo/MØ in breast cancer microenvironment and treated with SHA1 or sHA. TSG-6 protein levels detection (Free TSG-6 [∼35 kDa] and TSG-6/HC [∼120 kDa]), by western blot assay, in conditioned media of Mo/MØ treated with sHA1 or sHA3 in physiological and breast tumor context. Protein levels were semi quantified by densitometry from three independent experiments (a). Xenograft breast cancer model. nu/nu mice were injected with MDA-MB-231 cells and 9 days later, animals with similar tumor volumes were inoculated with Mo/MØ preincubated with sHA1 or sHA3. Tumors were fixed, and sections were stained with DAPI (blue, nuclei), TSG-6 (red) and HA (green) (top picture) or hematoxylin/eosin (H&E) and GSL-1 (green, endothelial cells) to analyze in vivo angiogenesis (bottom picture). Bars represent the average amount of TSG-6+, HA+ and GSL-1-FITC+ staining/field ± SEM from 10 representative visual fields (b). (*) $p < .05$, (**) $p < .01$ and (***) $p < .001$. Black asterisks indicate significant differences regard to basal control (BC); red asterisks indicate significant differences between treatments. MCM: MDA-MB-231 conditioned media (treated we sHA1, sHA3)

see Table 1) affect the behavior of immune cells, Mo/MØ or EC associated to a tumor context.

Therefore, the highlight of our work is that sHA, in a breast and lung tumor context, can induce an anti-angiogenic action on tumor cells and Mo/MØ, evidenced by the decrease of EC migration and angiogenic factor levels. Notably, the negative effect of sHA on the migration of EC is not observed in a physiological context, indicating a specific action in the tumor microenvironment. Multiple factors can affect their invasive capacity.[29] Tumor-associated cells and ECM might alter EC and the action of different molecules.[30] Thus, our results are an example that the tumor microenvironment should be considered to establish the antiangiogenic properties of molecules and cells. We could suggest that factors present in CM derived from tumor cells treated with sHA change the migratory behavior of ECs (shown in Figure 2b).

Moreover Mo/MØ exposed to these CM released factors also diminished the ECs migration.

Besides, in breast tumor cells, we found that sHA1 and sHA3 reduced cell viability, measured by MTS, but none of them affected the apoptosis or proliferation process. We only observed an enhanced cytotoxicity effect at the higher concentration of sHA3 in breast and lung cancer cell lines. This result indicates that cell viability is affected by necrosis of necrosis-like mechanism, independent of apoptotic events.[31] However, more profound studies will be required for determining the molecular process. In contrast, in lung tumor cells, sHA1 and sHA3 increased cell viability and showed an opposite effect in the proliferation rate induced by sHA3 We also observed a similar effect of both sHA in cell viability and proliferation of colorectal cancer cells. These results indicate that sHA effects are dependent on the type of tumor. In fact,
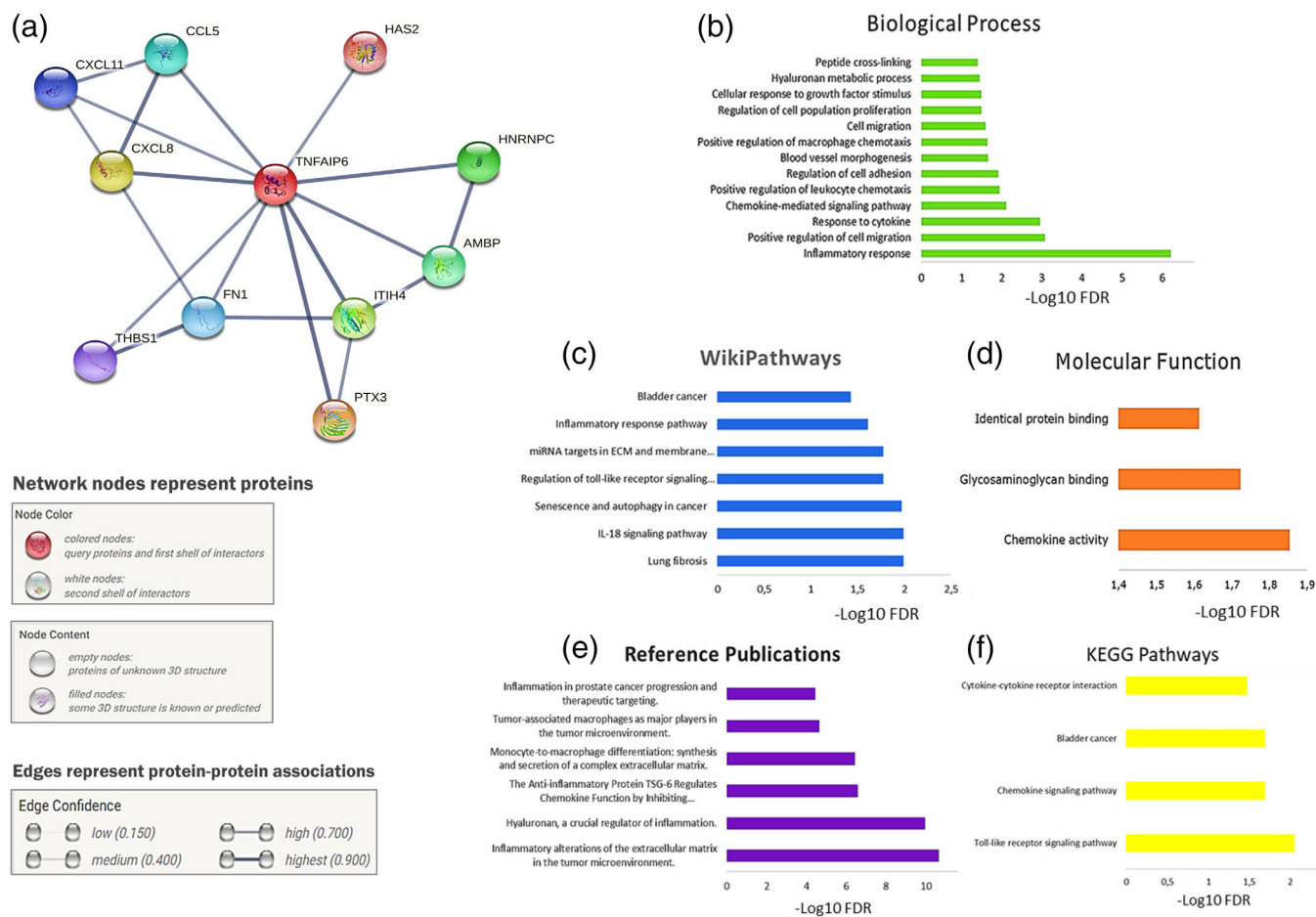
**FIGURE 8** In silico protein–protein interactions network (a) and enrichment analysis (b–f) generated by STRING v11 database for TSG-6. In (a), each node represents all the proteins produced by a single protein-coding gene locus and edges represent direct or indirect protein–protein associations. TSG-6 is shown as red node and interactions were predicted with a high confidence threshold of 0.7. In (b)–(f), functional enrichments significance was presented as—Log10 FDR (false discovery rate)

the 3D culture results showed that sHA1 and 3 reduced tumor sphere size in the TN breast and lung cancer cells but not in colorectal tumor cells.

When we analyzed the sHA effect on Mo/MØ we observed a differential effect between physiological and tumor context, depending on the tumor type. For instance, sHA3 and conditioned media (CM) of breast and lung tumor cells preincubated with sHA3 induced, on Mo/MØ, a decrease in migratory capacity, and mRNA expression of angiogenic factors (*VEGF*, *FGF-2*, and *IL-8*). Probably associated with a modulation of VEGF biosynthesis (as was observed a dismissed in sHA3 treated breast cancer cell line); or that sHA3 could affect VEGF, since sHA could affect its activity.[13]

Besides, the biosynthesis of TGF-1β, a key anti-inflammatory cytokine in the cancer milieu,[32] was reduced in Mo/MØ exposed to CM from breast and lung cancer cells treated with sHA3. These results suggest that sHA, particularly sHA3, affects the angiogenic and anti-inflammatory phenotype of Mo/MØ, acquiring a anti

tumoral side face.[18] However, this treatment with sHA3 and MCM on Mo/MØ increased the TSG-6·HC complex, where TSG-6 is associated with anti-inflammatory process.[21] We have previously reported that HMW HA induce proangiogenic behavior in Mo/MØ[20] and simultaneously decrease TSG-6·HC complex levels. Thus, it is possible to suggest that in a cancer microenvironment, TSG-6 directly affects non or sulfated HA function, and could directly action on angiogenesis. The TSG-6·HC protein complex, observed in Figure 7a, indicatives of the enzymatic activity of TSG-6 because TSG-6 catalyzes the transfer of the IαI HC to HA. This interaction affects the activity of the proteinase inhibitor,[33,34] the HA structure, its binding capacity to its receptors and its function.[35] In fact, HC·HA from human amniotic membranes could be potently antiangiogenic.[36] Furthermore, TSG-6 was found to inhibit the interaction of FGF2 and PTX3, restoring FGF2 proangiogenic activity.[21,37] In this sense, TSG-6 is not a direct promoter of angiogenesis, but it inhibits the inhibition of this process.[21] In our model, the modulation

of TSG-6·HC complex or the diminishing of free TSG-6 under MDA-MB-231 CM treated with sHA3 could reduce endogenous HA angiogenic action, indicating that sHA could also be associated with TSG-6 functions. Besides, it is possible to suggest that sHA also induce intracellular signal by the same receptors of endogenous HA, affecting this interaction by different mechanisms. It has been documented that MW and the sulfation of HA, change, or decrease the interaction with its main receptor CD44, without abolishing its binding.[38] For example, down-regulation of RHAMM or CD44, was observed in prostate cancer cell lines, resulting in a diminished PI3K/Akt signaling pathway.[12] Recently, Koutsakis et al.[15] have demonstrated that sHA (similar to our sHA) modulates the expression of HA synthase but not CD44 in breast cancer cells. Finally, when we used an in vivo xenograft breast cancer model, we found a significant decrease in vascularization in tumors inoculated with Mo/MØ pre-incubated with sHA1 or sHA3. These results concordance with the in vitro model, indicating that sHA has an antiangiogenic action in Mo/MØ in the breast tumor context. Alternatively, a reduction in the total levels of TSG-6 was found in tumors inoculated with Mo/MØ preincubated with sHA1 or sHA3, as well as a decrease in total HA. Moreover, with the results obtained in the in silico using the STRING analysis, we determined the network associated with TSG-6 and observed strong relations with proteins involved in inflammation, components of ECM, as fibronectin and hyaluronan metabolism, monocyte/macrophage differentiation and regulation of chemokine function. Reinforcing our hypothesis that sHA affect the enzymatic TSG-6 activity, modulates HA and, in turn, the tumor and associated cells, allowing the generation of an antitumoral and anti-angiogenic microenvironment in breast and lung tumors.

However, these findings require more studies to examine how sHA affects tumor cells' viability, which factors modulate or interact within the tumor context, for defining it as a new compound with antitumor properties. *In summary, this study showed for the first time that sHA, a molecule with low toxicity and high efficacy, has anti-angiogenic action in tumor cells and Mo/MØ in the breast and lung carcinoma milieu. These findings are of great interest since sHA seems to be a promising agent to complement and increase the success of chemoimmunotherapy used in the treatment of these types of cancer.*

## ORCID
*Laura Alaniz* https://orcid.org/0000-0002-6070-6078

## REFERENCES

1. Spinelli FM, Vitale DL, Demarchi G, Cristina C, Alaniz L. The immunological effect of hyaluronan in tumor angiogenesis. Clin Transl Immunol. 2015;4(12):e52.
2. Karamanos NK, Theocharis AD, Piperigkou Z, et al. A guide to the composition and functions of the extracellular matrix. FEBS J. 2021;288(24):6850–6912.
3. Day AJ, Prestwich GD. Hyaluronan-binding proteins: Tying up the giant. J Biol Chem. 2002;277(7):4585–4588.
4. Spinelli FM, Vitale DL, Sevic I, Alaniz L. Hyaluronan in the tumor microenvironment. Adv Exp Med Biol. 2020;1245:67–83.
5. Heldin P, Basu K, Olofsson B, Porsch H, Kozlova I, Kahata K. Deregulation of hyaluronan synthesis, degradation and binding promotes breast cancer. J Biochem. 2013;154(5):395–408.
6. Velesiotis C, Vasileiou S, Vynios DH. A guide to hyaluronan and related enzymes in breast cancer: Biological significance and diagnostic value. FEBS J. 2019;286(15):3057–3074.
7. Alaniz L, García MG, Gallo-Rodriguez C, et al. Hyaluronan oligosaccharides induce cell death through PI3-K/Akt pathway independently of NF-κB transcription factor. Glycobiology. 2006;16(5):359–367. doi:10.1093/glycob/cwj085
8. Toole BP. Hyaluronan: from extracellular glue to pericellular cue. Nat Rev Cancer. 2004;4(7):528–539.
9. Lokeshwar VB, Mirza S, Jordan A. Targeting hyaluronic acid family for cancer chemoprevention and therapy. Advances in cancer research. first ed. USA: Elsevier Inc., 2014; p. 35–65.
10. Pavan M, Beninatto R, Galesso D, et al. A new potential spreading factor: Streptomyces koganeiensis hyaluronidase. A comparative study with bovine testes hyaluronidase and recombinant human hyaluronidase of the HA degradation in ECM. Biochim Biophys Acta Gen Subj. 2016;1860(4):661–668.
11. Isoyama T, Thwaites D, Selzer MG, Carey RI, Barbucci R, Lokeshwar VB. Differential selectivity of hyaluronidase inhibitors toward acidic and basic hyaluronidases. Glycobiology. 2006;16(1):11–21.
12. Benitez A, Yates TJ, Lopez LE, Cerwinka WH, Bakkar A, Lokeshwar VB. Targeting hyaluronidase for cancer therapy: Antitumor activity of sulfated hyaluronic acid in prostate cancer cells. Cancer Res. 2011;71(12):4085–4095.
13. Jordan AR, Lokeshwar SD, Lopez LE, et al. Antitumor activity of sulfated hyaluronic acid fragments in pre-clinical models of bladder cancer. Oncotarget. 2017;8(15):24262–24274.
14. Lim DK, Wylie RG, Langer R, Kohane DS. Selective binding of C-6 OH sulfated hyaluronic acid to the angiogenic isoform of VEGF165. Biomaterials. 2016;77:130–138.

15. Koutsakis C, Tavianatou A-G, Kokoretsis D, Baroutas G, Karamanos NK. Sulfated hyaluronan modulates the functional properties and matrix effectors expression of breast cancer cells with different estrogen receptor status. Biomol Ther. 2021; 11(12):1916.

16. Bussard KM, Mutkus L, Stumpf K, Gomez-Manzano C, Marini FC. Tumor-associated stromal cells as key contributors to the tumor microenvironment. Breast Cancer Res. 2016; 18(1):84.

17. Mantovani A, Marchesi F, Malesci A, Laghi L, Allavena P. Tumour-associated macrophages as treatment targets in oncology. Nat Rev Clin Oncol. 2017;14:399–416.

18. Hao N-B, Lü M-H, Fan Y-H, Cao Y-L, Zhang Z-R, Yang S-M. Macrophages in tumor microenvironments and the progression of tumors. Clin Dev Immunol. 2012;2012:1–11.

19. Rayahin JE, Buhrman JS, Zhang Y, Koh TJ, Gemeinhart RA. High and low molecular weight hyaluronic acid differentially influence macrophage activation. ACS Biomater Sci Eng. 2015; 1(7):481–493.

20. Spinelli FM, Vitale DL, Icardi A, et al. Hyaluronan preconditioning of monocytes/macrophages affects their angiogenic behavior and regulation of TSG-6 expression in a tumor type-specific manner. FEBS J. 2019;286(17):3433–3449.

21. Day AJ, Milner CM. TSG-6: A multifunctional protein with anti-inflammatory and tissue-protective properties. Matrix Biol. 2019;78–79:60–83.

22. Hintze V, Moeller S, Schnabelrauch M, et al. Modifications of Hyaluronan influence the interaction with human bone morphogenetic protein-4 (hBMP-4). Biomacromolecules. 2009; 10(12):3290–3297.

23. Weischenfeldt J, Porse B. Bone marrow-derived macrophages (BMM): Isolation and applications. Cold Spring Harb Protoc. 2008;2008(12): pdb.prot5080.

24. Kapałczyńska M, Kolenda T, Przybyła W, et al. 2D and 3D cell cultures - A comparison of different types of cancer cell cultures. Arch Med Sci. 2018;14(4):910–919.

25. Fujimoto T, Savani RC, Watari M, Day AJ, Strauss JF. Induction of the hyaluronic acid-binding protein, tumor necrosis factor-stimulated gene-6, in cervical smooth muscle cells by tumor necrosis factor-α and prostaglandin E2. Am J Pathol. 2002;160(4):1495–1502.

26. Pasarica M, Sereda OR, Redman LM, et al. Reduced adipose tissue oxygenation in human obesity. Diabetes. 2009;58(3): 718–725.

27. Szklarczyk D, Gable AL, Lyon D, et al. STRING v11: Protein–protein association networks with increased coverage, supporting functional discovery in genome-wide experimental datasets. Nucleic Acids Res. 2019;47(D1):D607–D613.

28. Koehler L, Ruiz-Gómez G, Balamurugan K, et al. Dual action of sulfated Hyaluronan on Angiogenic processes in relation to vascular endothelial growth factor-A. Sci Rep. 2019;9(1): 1–18.

29. Cheresh DA, Stupack DG. Regulation of angiogenesis: Apoptotic cues from the ECM. Oncogene. 2008;27(48):6285–6298.

30. Hida K, Maishi N, Annan DA, Hida Y. Contribution of tumor endothelial cells in cancer progression. Int J Mol Sci. 2018; 19(5):1272.

31. Nirmala JG, Lopus M. Cell death mechanisms in eukaryotes. Cell Biol Toxicol. 2020;36(2):145–164.

32. Caja L, Dituri F, Mancarella S, et al. TGF-β and the tissue microenvironment: Relevance in fibrosis and cancer. Int J Mol Sci. 2018;19(5):1294.

33. Briggs DC, Birchenough HL, Ali T, et al. Metal ion-dependent heavy chain transfer activity of TSG-6 mediates assembly of the cumulus-oocyte matrix. J Biol Chem. 2015 Nov;290(48):28708–28,723.

34. Rugg MS, Willis AC, Mukhopadhyay D, et al. Characterization of complexes formed between TSG-6 and inter-α-inhibitor that act as intermediates in the covalent transfer of heavy chains onto hyaluronan. J Biol Chem. 2005;280(27):25674–25686.

35. Day AJ, de la Motte CA. Hyaluronan cross-linking: A protective mechanism in inflammation? Trends Immunol. 2005; 26(12):637–643.

36. Yan T, Chen X, Zhan H, et al. Interfering with hyaluronic acid metabolism suppresses glioma cell proliferation by regulating autophagy. Cell Death Dis. 2021;12(5):486.

37. Leali D, Inforzato A, Ronca R, et al. Long pentraxin 3/tumor necrosis factor-stimulated gene-6 interaction: A biological rheostat for fibroblast growth factor 2-mediated angiogenesis. Arterioscler Thromb Vasc Biol. 2012;32(3):696–703.

38. Bhattacharya DS, Svechkarev D, Souchek JJ, et al. Impact of structurally modifying hyaluronic acid on CD44 interaction. J Mater Chem B. 2017;5(41):8183–8192.

## SUPPORTING INFORMATION

Additional supporting information may be found in the online version of the article at the publisher's website.